Striatal Crosstalk Between Dopamine and Serotonin Systems

Authors: Yu Liu[1], Juan Enriquez Traba[1] and Christian Lüscher*[1,2,3]

Affiliations:

[1] Department of Basic Neurosciences, Medical Faculty, University of Geneva, CH-1211 Geneva, Switzerland.

[2] Clinic of Neurology, Department of Clinical Neurosciences, Geneva University Hospital, CH-1211 Geneva, Switzerland.

[3] Synapsy Center for Mental Health Research, University of Geneva, CH-1211 Geneva, Switzerland

* Corresponding author email: christian.luscher@unige.ch

Abstract:

Dopamine (DA) and serotonin (5-HT) are neuromodulators in reward processing, decision-making, and motivated behavior. While often viewed as opposing or complementary systems, how DA and 5-HT release integrate in the striatum remains elusive. Using optogenetics, fiber photometry, and slice electrophysiology, we found that ventral tegmental area (VTA) DA neuron stimulation increased DA release without affecting 5-HT release. Dorsal raphe nucleus (DRN) 5-HT neuron activation, on the other hand, induced serotonin release and a transient increase in DA in the NAc, likely via glutamate co-release onto VTA DA neurons during the initial stimulation phase. These findings indicate that DA and 5-HT operate largely independently in the striatum, with selective circuit-dependent interactions. This work refines our understanding of DA-5HT interactions and provides a foundation for future research into their roles in motivated behaviors and neuropsychiatric disorders.

Main Text:

DA neurons projecting from the VTA to the striatum [1-3] are involved in various cognitive functions, and DA dysregulation has been associated with several neuropsychiatric and neurodegenerative disorders [4-7]. Tryptophan-hydroxylase-positive (TpH+) neurons synthesize 5-HT in the dorsal raphe nucleus (DRN) and modulates synaptic transmission in the VTA, NAc and DS. Behavioral and pharmacological studies suggest that 5-HT, acting in concertation with DA, may affect reward-seeking, decision making, associative learning, and motor planning [8, 9].

Two conflicting hypotheses regarding the interaction between the DA and 5-HT systems exist. The opponency hypothesis [10-12] suggests that DA and 5-HT have opposite functions: while DA promotes behavioral activation, 5-HT, by contrast, suppresses behavior. Pharmacological studies indicate DA and 5-HT agonists or antagonists have opposite effects on reward processing [13, 14], feeding behavior [14], and self-stimulation [15]. Recent *in vivo* fiber photometry recordings further support this oppositional dynamic, suggesting that DA and 5-HT exhibit inverse activity patterns in the striatum in response to reward [16] and following choice actions [17]. Moreover, 5-HT can inhibit DA activity in the VTA and substantia nigra, leading to reduced DA release in the striatum[10, 18].

Alternatively, 5-HT could directly enhance DA activity or share properties that facilitate reinforcement processing similar to DA. Local 5-HT infusion into the striatum can increase extracellular DA levels [19]. Additionally, 5-HT can facilitate DA's behavioral effects. For example, selective serotonin reuptake inhibitors (SSRIs) increase 5-HT, and lead to a modulative effect in DA self-stimulation thresholds [20] and enhancement of cocaine's reinforcing effects [21]. In contrast, depletion of 5-HT or its precursor blocks cocaine's rewarding effects [22], and impair d-amphetamine's ability to decrease impulsivity [23]. Furthermore, serotonergic activity in the dorsal raphe interacts with DA, encoding complementary aspects of reward processing [24].

The above-listed discrepancies suggest complex mechanisms underlying DA-5-HT crosstalk that remain largely elusive, underscoring a complex interplay driven by receptor-specific interactions and overlapping projections. For example, 5-HT modulation of DA activity occurs through 5-HT1A, 5-HT1B, and 5-HT2A receptor activation, which enhances DA release in the striatum and prefrontal cortex. In contrast, 5-HT2C receptor activity inhibits

DA release in mesolimbic regions [25].Additionally, lesion of DA neurons decreases 5HT spontaneous firing in DRN, whereas lesion of 5-HT neurons enhanced the firing activity of DA neurons in VTA [26].

Both DA and 5-HT are involved in reinforcement and decision-making in opposing and complementary ways [27]. An imbalance between these systems is implicated in various psychiatric disorders, including depression, schizophrenia, compulsion, and addiction [28-30]. However, these interactions are complex and not simply oppositional or coherent, requiring further investigation into their synaptic crosstalk and plasticity mechanisms.

There is increasing recognition of the functional and anatomical overlap between VTA DA neurons and DRN 5-HT neurons, particularly in the striatum, where both systems have dense projections and colocalizations [16, 31]. However, few studies have addressed the bidirectional interactions between the DA and 5-HT systems in response to specific neuronal stimulation, and the interaction between dorsal raphe (DR) serotonergic neurons and striatal DA transmission remains controversial. To address this gap, we investigated the effects of selective activation of DA and serotonin neurons on both DA and 5-HT release in the striatum. Recent advancements in GPCR sensors and refined optogenetic tools allow for real-time observation of neurotransmitter dynamics, enabling targeted interventions and establishing causal links. By stimulating DA neurons in the VTA and 5-HT neurons in the DRN, we aimed to investigate the reciprocal interactions between these systems and elucidate their crosstalk mechanisms.

Our findings demonstrate that stimulation of DA neurons in the VTA alters DA but not 5-HT release in the striatum, suggesting that the 5-HT system in the striatum operates relatively independently of VTA DA activity. In contrast, stimulation of 5-HT neurons in the DRN impacts mainly 5-HT with a minor impact on DA levels in the striatum, highlighting the reciprocal regulatory effects of serotonergic activity on DA circuits. These results provide new insights into the striatum's bidirectional interplay between DA and 5-HT systems.

Understanding the mechanisms underlying DA-5-HT crosstalk is critical for advancing our knowledge of neuromodulatory systems and developing therapeutic interventions for disorders characterized by imbalances in these networks. By simultaneously assessing DA and 5-HT release in response to targeted neuronal activation, this study contributes to a more comprehensive understanding of how these systems interact to regulate striatal function.

Results:

Activating VTA DA neurons increases DA but not 5HT in the striatum

We tested whether optogenetic stimulation of VTA DA neurons results in DA and/or 5-HT in the striatum. We injected AAV-FLEX-ChrimsonR-tdTomato into the VTA of DAT-Cre mice and AAV-dLight X.XX or AAV-GRAB5HT in the NAc or DS to monitor DA or 5-HT levels in the striatum (Figure 1B, C). We found that optogenetic stimulation of VTA DA neurons (Figure 1A) evoked a rapid and robust release of DA in NAc and DS, at a level within the same range as DA increase evoked by passive cocaine injection at 15mg/kg (Figure 1D). Conversely, we did not observe any change in 5-HT levels in either NAc or DS in response to VTA DA stimulation. In contrast, cocaine readily increased 5-HT levels in the two striatal regions (Figure 1G). These findings contradict the finding that optogenetic stimulation of serotonergic neurons in the DRN led to increased DA concentration in the striatum, as measured by microdialysis [31]. These conflicting results may arise from differences in stimulation protocols, measurement modalities, neuronal subpopulations recruited, or variations in experimental conditions, highlighting the complexity of 5-HT-DA interactions in the striatum. Together, these results suggest that VTA DA neurons modulate DA release but not 5-HT release in the striatum.

Activating DRN SERT neurons increases 5HT and transiently DA in the striatum.

Then, we tested whether stimulation of DRN SERT neurons produces a release of DA or 5-HT in the striatum (Figure 2B). We tested the effects of DRN SERT optogenetic stimulation. We found optogenetic stimulation of DRN SERT neurons evoked rapid and robust release of 5-HT in DS at a level that is comparable to the DA increase evoked by passive cocaine injection at 15mg/kg (Figure 2C). On the contrary, we did not observe any significant change in DA levels in either NAc or DS in response to DRN SERT stimulation. In contrast, cocaine could readily increase 5-HT levels in the two regions (Figure 2E).

Some studies have reported that electrical stimulation of the DRN inhibits DA neuron activity, suggesting a suppressive influence on DA release[32-34], whereas other findings report that electrical stimulation of the DRN induces DA release in the NAc [35]. We observed a small and transient increase in DA levels in NAc after DR SERT stimulation (Figure 2C, insert), significantly different from the baseline 5 seconds after the stimulation (Figure 2D).

Glutamate-5HT co-release of DR afferents in the VTA.

To further investigate this transient crosstalk, we examined the synaptic afferents onto midbrain and striatal neurons in the acute slice preparation, as DR projections have been claimed to release glutamate in addition to serotonin (REF). Combining optogenetic projection targeting and whole-cell recordings (Figure 3A) allowed parsing the synaptic currents in identified regions. Glutamatergic innervation was absent in DS (Figure 3B) and anterior NAc Shell (Figure 3C) but observed in OFC (Figure 3D) and posterior NAc Shell (Figure 3E), as well as the VTA (Figure 3F). These results suggest that DRN SERT neurons modulate 5-HT releases in the striatum and indirectly affect DA release. This might be explained by the 5-HT neurons projecting from the DRN also sending glutamatergic projections to VTA, stimulating DA neurons and causing a brief release of DA in the striatum.

Discussion:

Our findings demonstrate that optogenetic stimulation of DRN SERT and VTA DA neurons results in minimal crosstalk between striatal DA and 5-HT, indicating that these neurotransmitter systems operate largely independently. This challenges earlier studies that reported DRN stimulation increases striatal DA [31] — a discrepancy likely due to differences in measurement techniques. Microdialysis combined with HPLC may fail to fully distinguish 5-HT from DA because 5-HT shares similar physicochemical properties and overlapping electrochemical signals with 3-methoxytyramine (3-MT, a metabolite of DA)[36].

We employed advanced GPCR-based sensors with high selectivity and sensitivity to overcome these limitations, ensuring a more accurate assessment of neurotransmitter dynamics [37, 38]. Stimulation of DRN SERT neurons elicited a robust, rapid increase in striatal 5-HT levels—comparable to the DA surge induced by cocaine—yet did not significantly alter DA levels in the NAc or DS, except for a transient increase in the NAc. This modest DA change is consistent with previous findings[35] and may be explained by DRN 5-HT neurons projecting to the VTA and co-release glutamate, which can also excite VTA DA neurons and evoke DA release in NAc .

Moreover, our analysis revealed that the 5-HT-glutamate co-release mechanism was present in the OFC and posterior NAc shell but absent in the DS and anterior NAc shell, underscoring the region-specific effects of DRN SERT activation. Our results refine the understanding of DArgic and serotonergic interactions in the striatum, highlighting their functionally distinct roles. These insights provide a foundation for future research into the interplay between these systems in cognitive and behavioral functions, with implications for neuropsychiatric disorders.

Methods

Animals:

DAT-IRES-Cre (B6.SJL-Slc6a3$^{tm1.1(cre)Bkmn}$/J) and SERT-Cre mice (B6.129(Cg)-Slc6a4tm1(cre)Xz/J) were from the Jackson Laboratory. Upon the arrival of the animals a period of 7 days of habituation was made. Both male and female mice aged from 8-12 weeks were used and group housed in a temperature and humidity-controlled environment, under a 12 h light/dark cycle, and provided with food and water *ad libitum*.Weights and genders were distributed homogeneously among the groups if possible. All behavioral procedures were performed during the light cycle. All procedures were approved by the Institutional Animal Care and Use Committee of the University of Geneva and by the animal welfare committee of the Cantonal of Geneva, in accordance with Swiss law (GE131A_33975).

Virus injection and implantation:

Mice (age 8-12 weeks) were deeply anesthetized with a mixture of Isoflurane (w/v, induction 5%, maintenance 2%, Attane^{tm}) and O_2 (Compact anesthesia station from Minerve) during surgery and then secured in a stereotaxic frame (Angle One). Before craniotomy, body temperature was maintained at 37 °C with a temperature controller system and Lacryvisc (Alcon, Switzerland) was applied to prevent the eyes from drying. Lidocaine was applied on the surface of the epicranium. An incision was made to expose the bregma and lambda point of the skull. The skull above the target area was thinned with a dental drill and carefully removed. Viruses were injected with glass pipette at a rate of 50 nl/min. The amount of virus per injection site was 350-500 nl. After injection, the pipette was left in the place for 10 min to allow diffusion of the virus. The skin was sutured and disinfected after the injection. 500 µl saline was i.p. injected. Paracetamol (2 mg/ml in the water bottle) was given orally for the next 2-4 days.

(anterior posterior (AP): −3.28; medio–lateral (ML): −0.9; dorso-ventral (DV): -4.3; with a 10° angle)

To express opsins, AAV8-syn-Flex-Chrimson-tdTomato (UNC) was injected in VTA (anterior posterior (AP): −3.28; medio–lateral (ML): −0.9; dorso-ventral (DV): -4.3; with a 10° angle) of DAT-Cre mice or DRN (AP: −4.5; ML: 0; DV: −3) of SERT-Cre mice. To record DA release, an AAV5-CAG-dLight1.2 (400 nl, from Addgene) was injected in NAc (AP: +1.6; ML: ±0.75; DV: -4.3) and DS (AP: +1.3; ML: ±0.1; DV: -3.3). To record 5-HT release, AAV9-hSyn-5-HT3.0 (400 nl, from BrainVTA) was injected in NAc (AP: +1.6; ML: ±0.75; DV: -4.3) and DS (AP: +1.3; ML: ±0.1; DV: -3.3).

During the same surgical procedure, three screws were fixed into the skull to secure the optical implant. An optic fiber (0.4 mm diameter, MFC_400/430_0.48_4mm_ZF2.5(G)FLT, Doric Lenses) was implanted 150 µm above the virus injection site for in vivo fiber photometry recording. Another optic fiber (0,2 mm diameter, FOC-W-1.25-200-0.37-5.0, Inper) was implanted 200 µm above the virus injection site for optogenetic stimulation. Then the optic fibers were fixed to the skull with dental cement. After surgery mice were given 7 days of recovery and were habituated to handling.

For electrophysiological studies examining DRN SERT connectivity, AAV8-syn-Flex-Chrimson-tdTomato (UNC) was injected in DRN (AP: −4.5; ML: 0; DV: −3) of SERT-Cre mice.

Behavioral Paradigm:

After 4-5 week of viral expression, mice were habituated to handling and to the connection cable for three day before testing. On the testing day mice were connected to the optogenetics cable and fiber photometry cable and placed in a transparent custom build open-field (30 X 30 X 20 cm) for 3 min of habituation before the start of recording. Then, 5 min of baseline recording were made. Animal received 5 pulses of laser stimulations, each composed of 30 bursts separated by 250 ms (each burst consisted of 5 laser pulses of 4-ms pulse width at 20 Hz). After another 5 minutes of baseline recording, animals received i.p. injection of cocaine (15mg/kg), and the neuronal activity was recorded for another 40 minutes.

Optogenetic stimulation:

Optic fiber for optogenetic stimulation of mice were connected via patch cords (MFO-F-W1.25-200-0,37-100, Inper) to a rotary joint (FRJ_1 × 2_FC-2FC; Doric Lenses, Quebec, Canada), suspended above the operant chamber. A second patch cord was connected from the rotary joint to an orange DPSS laser (SDL-593–100 mW; Shanghai Dream Lasers; Shanghai, China) positioned outside of the context. Laser power was typically 15–20 mW measured at the end of each patch cord. A mechanical shutter was used to control laser output (SR474 driver with SR476 shutter head; Stanford Research Systems, aligned using a connectorized mechanical shutter adaptor; Doric Lenses).

Fiber Photometry recordings:

Fiber photometry was performed similar to before (33). During recordings, excitation (470 nm, M470F3, Thorlabs) and control LED light (405 nm, M405FP1, Thorlabs) was passed

through excitation filters and focused onto a patch cord. Both LED lights were sinusoidally modulated at 211 and 531 Hz (470 nm and 405 nm light, respectively) and light was passed through a mini cube (FMC4_AE(405)_E(450-490)_F(500-550)_S) onto the optic fiber patch cable (MFP_400/430/1100–0.48_4 m_FC-ZF2.5, Doric Lenses) that was connected to the chronically implanted fiber (MFC_400/430- 0.48_6mm_ZF2.5(G)_FLT, Doric Lenses). Light intensity at the tip of the patch cable was around 0.25 mW. Emission light travelled back through the same

fibers onto the mini cube and a photo-receiver (Newport 2151, Doric Lenses), after which it was digitized, demodulated and stored using a signal processor (RZ5P, Tucker Davis Technologies).

The sample rate was 101.725 Hz, signals were low-pass filtered online at 3 Hz.

The data were analyzed using MATLABR2024 (MathWorks). First the signal during baseline acquisition originating from the 405 nm excitation source was linearly regressed to the signal originating from the 470 nm excitation source, and scale to the 470 nm originating signal. $\Delta F/F$ was then computed as (470 nm signal – fitted 405 nm signal)/fitted 405 nm signal. The average $\Delta F/F$ signal in the baseline periods before experimental intervention was then subtracted to normalize the signal to baseline. Finally, the normalized signal was binned into appropriate time bins in the graphs and analyses.

<u>Electrophysiology recording ex vivo</u>

SERT-Cre mice were injected with AAV-FLEX-Chirmsom-tdT in the DRN to detect potential glutamate corelease from 5-HT neurons. Three weeks after injection, mice were deeply anesthetized with 5% isoflurane and subsequently decapitated after confirmation of absent of toe and tail reflexes.

92 mM NMDG, 20 mM HEPES, 25 mM glucose, 30 mM NaHCO3, 2.5 mM KCl, 1.2 mM NaH2PO4 (pH 7.35, 303–306 mOsm) and saturated with 95% O2/5% CO2. Coronal slices (300 µm) containing the OFC, DS, NAc anterior, NAc posterior and VTA were prepared at a speed of 0.07 mm/s using a vibratome (Leica, VT1200). After slicing, sections were allowed to recover at 34°C in bubbled NMDG-based for 5-10 min, before being transferred to a holding chamber filled with modified holding aCSF saturated with 95% O2/5% CO2 containing 92 mM NaCl, 20 mM HEPES, 25 mM glucose, 30 mM $NaHCO_3$, 2.5 mM KCl, 1.2 mM $NaPO_4$ (pH 7.35, 303–306 mOsm) at room temperature for at least 1 h.

For recordings, slices were kept at 30 °C in a recording chamber perfused with 1.5 – 2.0 ml/min ACSF containing 126 mM NaCl, 2.5 mM KCl, 1.4 mM NaH_2PO_4, 1.2 mM $MgCl_2$, 2.4 mM $CaCl_2$, 25 mM $NaHCO_3$ and 11 mM glucose (303–305 mOsm). Neurons were visualized with a ×40 water-immersion objective on an Olympus BX5iWI inverted microscope equipped with infrared-differential interference contrast (IR-DIC) optics and epifluorescence (Olympus Corp). Td-tomato-positive cells were classified based on strong fluorescence, while td-tomato-negative cells were those adjacent to td-tomato-positive cells, but lacking fluorescence. Whole cell recordings were amplified (Multiclamp 700B, Axon Instruments), filtered at 5 kHz and digitized at 20 kHz (National Instruments Board PCI-MIO-16E4, Igor, Wave Metrics). Data were rejected if the access resistance changed more than 20%. Optogenetic EPSCs were evoked with single or paired pulses of 0.1 Hz, with an interstimulus interval of 50 ms.), and recorded in the presence of PTX (100 µM, Tocris).

Histological analysis:

Brains were fixed with 4% paraformaldehyde (PFA) for at least 24 h and sliced with vibratome (Leica, VT1200). 50 µm thick slices were washed with 3 times PBS for 5 min and blocked with 10% bovine serum albumin (BSA) dissolved in 0.5% TritonX-100 for 1 hour at room temperature. Slices were incubated with primary antibodies dissolved in blocking buffer overnight at 4 , followed by 4 times 15 min wash with PBS at room temperature. After that, slices were incubated with fluorescent-conjugated secondary antibodies dissolved in blocking buffer for 2 h at room temperature followed by 4 times 15 min wash with PBS. Last, slices were mounted using mounting medium containing DAPI (Fluoroshiel, Abcam). Primary and secondary antibodies are listed below: Rabbit anti GFP (1:500, Invitrogen, A11122, RRID: AB_221569); Goat anti Rabbit 488 (1:500, Invitrogen, A11008, RRID: AB_143165).

Statistical analysis:

Statistical analysis was performed in GraphPad Prism 9. For all tests, the significance threshold was placed at $\alpha = 0.05$. Gaussian distribution was evaluated using D'Agostino & Pearson normality test. Multiple comparisons were first subject to mixed-factor ANOVA defining both between- and/or within-group factors. Where significant main effects or interaction between factors were found ($P < 0.05$), further comparisons were

made by a two-tailed Student's t-test with Bonferonni corrections applied when appropriate (that is, the level of significance equaled 0.05 divided by the number of comparisons). Mann-Whitney or Friedman test were used for non-Gaussian distributions when appropriate. Single comparisons of between- or within-group measures were made by two-tailed non-paired or paired Student's t-test, respectively.

Acknowledgments: We thank all the Lüscher lab members for their comments on the manuscript. This work was supported by the Swiss National Science Foundation (grant no. 310030_219470) and European Union's Horizon 2020 Research and Innovation Program DEEPER project (grant no. 101016787) to C.L.

Author information:

Conceptualization: YL, CL

Investigation: YL, JET

Formal Analysis: YL, JET

Visualization: YL, CL, JET

Funding acquisition: CL

Supervision: CL

Writing – original draft: YL, CL

Writing – review & editing: YL, CL, JET

Competing interests:

The authors declare no competing interests.

Materials & correspondence:

Corresponding author email: christian.luscher@unige.ch

Fig 1. Stimulation of VTA DA system increases DA but not 5-HT level in the striatum. (**A**) Protocol of optogenetic stimulations and cocaine treatments. (**B**) Schematic of virus injection sites and optic fiber implantation sites for VTA stimulation in DAT-cre mices. (**C**) (Left) dLight expression and photometry fiber placement in the NAc co-labeled with tdTomato projection from VTA. (Middle) dLight expression and photometry fiber placement in the DS co-labeled with tdTomato projections from VTA. (Right) Optogenetic stimulation fiber placement and Chrimson-tdT expression in the VTA. Scale bars, 1 mm. (**D**) DA increases after optogenetic stimulation of VTA DA neurons (left) and i.p. cocaine injections (right) in NAc (red trace, n = 6) and DS (blue trace, n = 5). (**E**) Area under curve of DA signal in NAc and DS in 5 seconds during baseline and after optogenetic stimulation (Wilcoxon test; NAc: W = 21, z = 0.765, *P = 0.016, n = 6 mice; DS: W = 15, z = 0.198, *P = 0.031; n = 5 mice respectively). (**F**) Ratio of peak DA signal after optogenetic stimulation and peak DA signal after cocaine injection. (**G**) 5-HT increases after optogenetic stimulation of VTA DA neurons (left) and i.p. cocaine injections (right) in NAc (red trace, n = 4) and DS (blue trace, n = 6). (**H**) Area under curve of DA signal in DS in 5 seconds during baseline and after optogenetic stimulation (Wilcoxon test; NAc: W = 2, z = -0.01, P = 0.375, n = 3 mice; DS: W = 3, z = 0.00, P = 0.422, n = 6 mice respectively). (**I**) Ratio of peak 5-HT signal after optogenetic stimulation and peak 5-HT signal after cocaine injection.

Fig 2. Stimulation of DRN 5-HT system increases 5-HT but not DA level in the striatum. (**A**) Schematic of virus injection sites and optic fiber implantation sites for DR stimulation in SERT-cre mice. (**B**) (Left) GRAB-5HT expression and photometry fiber placement in the NAc co-labeled with tdTomato projection from DR. (Middle) GRAB-5HT expression and photometry fiber placement in the DS co-labeled with tdTomato projections from DR. (Right) Optogenetic stimulation fiber placement and Chrimson-tdT expression in the DR. Scale bars, 1 mm. (**C**) DA increases after optogenetic stimulation of DR SERT neurons (left) and i.p. cocaine injections (right) in NAc (red trace, n = 4) and DS (blue trace, n = 4). (**D**) The area under the curve of DA signal in NAc and DS in 5 seconds during baseline and after optogenetic stimulation. (Wilcoxon test; NAc: W = 15, z = 0.05, *P = 0.031, n = 5 mice; DS: W = 8, z = 0.038, P = 0.125, n = 4 mice respectively). (**E**) Ratio of peak DA signal after optogenetic stimulation and peak DA signal after cocaine injection. (**F**) 5-HT increases after optogenetic stimulation of DR SERT neurons (left) and i.p. cocaine injections (right) in DS (blue trace, n = 2). (**G**) Area under curve of 5-HT signal in DS in 5 seconds during baseline and after optogenetic stimulation. (Wilcoxon test; DS: W = 15, z = 0.423, *P = 0.031, n = 4 mice respectively). (**H**) Ratio of peak 5-HT signal after optogenetic stimulation and peak 5-HT signal after cocaine injection.

Fig 3. DRN 5HT neurons make excitatory synapses onto OFC, pNAcSh, and VTA neurons.

(**A**) Top: Diagram of virus injection of AAV-Syn-FLEX-Chrimson-tdTomato in the DRN of SERT-Cre mice. Bottom: Representative image of tdTomato–expressing cell bodies of Sert neurons in the DRN. Scale bar, 200 uM. (**B-F**) Top: Localization of recordings in the DS (B), NAcSh anterior (C), OFC(D), NAcSh posterior (E) and VTA (F). Bottom: representative traces of p-pulse optical stimulation of Chrimsom+ fibers, before and after bath application of NBQX/AP5 (20 mM) in OFC (C), NAcSh posterior (D) and VTA (E) neurons. (**G-I**): Quantification of the amplitude of responses before and after NBQX/AP5 bath-application.

References and Notes

1. Robinson, T.E. and K.C. Berridge, *The neural basis of drug craving: an incentive-sensitization theory of addiction*. Brain research reviews, 1993. **18**(3): p. 247-291.
2. Horvitz, J.C., *Mesolimbocortical and nigrostriatal dopamine responses to salient non-reward events*. Neuroscience, 2000. **96**(4): p. 651-656.
3. Haber, S.N., J.L. Fudge, and N.R. McFarland, *Striatonigrostriatal pathways in primates form an ascending spiral from the shell to the dorsolateral striatum.* J Neurosci, 2000. **20**(6): p. 2369-82.
4. Di Chiara, G. and A. Imperato, *Drugs abused by humans preferentially increase synaptic dopamine concentrations in the mesolimbic system of freely moving rats*. Proceedings of the National Academy of Sciences, 1988. **85**(14): p. 5274-5278.
5. Schultz, W., *Multiple dopamine functions at different time courses.* Annu. Rev. Neurosci., 2007. **30**(1): p. 259-288.
6. Ikemoto, S., *Brain reward circuitry beyond the mesolimbic dopamine system: A neurobiological theory*. Neuroscience & Biobehavioral Reviews, 2010. **35**(2): p. 129-150.
7. Pascoli, V., et al., *Sufficiency of mesolimbic dopamine neuron stimulation for the progression to addiction.* Neuron, 2015. **88**(5): p. 1054-1066.
8. Lucki, I., *The spectrum of behaviors influenced by serotonin.* Biol Psychiatry, 1998. **44**(3): p. 151-62.
9. Barton, D.A., et al., *Elevated brain serotonin turnover in patients with depression: effect of genotype and therapy*. Archives of General Psychiatry, 2008. **65**(1): p. 38-46.
10. Daw, N.D., S. Kakade, and P. Dayan, *Opponent interactions between serotonin and dopamine.* Neural networks, 2002. **15**(4-6): p. 603-616.
11. Rogers, R.D., *The Roles of Dopamine and Serotonin in Decision Making: Evidence from Pharmacological Experiments in Humans.* Neuropsychopharmacology, 2011. **36**(1): p. 114-132.
12. Boureau, Y.L. and P. Dayan, *Opponency Revisited: Competition and Cooperation Between Dopamine and Serotonin.* Neuropsychopharmacology, 2011. **36**(1): p. 74-97.
13. Fletcher, P.J., Z.-H. Ming, and G.A. Higgins, *Conditioned place preference induced by microinjection of 8-OH-DPAT into the dorsal or median raphe nucleus.* Psychopharmacology, 1993. **113**(1): p. 31-36.
14. Fletcher, P.J., K.M. Korth, and J.W. Chambers, *Selective destruction of brain serotonin neurons by 5,7-dihydroxytryptamine increases responding for a conditioned reward.* Psychopharmacology, 1999. **147**(3): p. 291-299.
15. Fletcher, P.J., M. Tampakeras, and J.S. Yeomans, *Median raphe injections of 8-OH-DPAT lower frequency thresholds for lateral hypothalamic self-stimulation.* Pharmacology Biochemistry and Behavior, 1995. **52**(1): p. 65-71.
16. Cardozo Pinto, D.F., et al., *Opponent control of reinforcement by striatal dopamine and serotonin.* Nature, 2024.
17. Bang, D., et al., *Sub-second Dopamine and Serotonin Signaling in Human Striatum during Perceptual Decision-Making*. Neuron, 2020. **108**(5): p. 999-1010.e6.
18. Kapur, S. and G. Remington, *Serotonin-dopamine interaction and its relevance to schizophrenia.* Am J Psychiatry, 1996. **153**(4): p. 466-76.
19. De Deurwaerdère, P., et al., *Serotonin enhances striatal dopamine outflow in vivo through dopamine uptake sites*. J Neurochem, 1996. **66**(1): p. 210-5.
20. Harrison, A.A. and A. Markou, *Serotonergic Manipulations Both Potentiate and Reduce Brain Stimulation Reward in Rats: Involvement of Serotonin-1A Receptors.*

The Journal of Pharmacology and Experimental Therapeutics, 2001. **297**(1): p. 316-325.

21. Sasaki-Adams, D.M. and A.E. Kelley, *Serotonin-Dopamine Interactions in the Control of Conditioned Reinforcement and Motor Behavior.* Neuropsychopharmacology, 2001. **25**(3): p. 440-452.
22. Aronson, S.C., et al., *Serotonergic mechanisms of cocaine effects in humans.* Psychopharmacology, 1995. **119**(2): p. 179-185.
23. Winstanley, C.A., et al., *Interactions between Serotonin and Dopamine in the Control of Impulsive Choice in Rats: Therapeutic Implications for Impulse Control Disorders.* Neuropsychopharmacology, 2005. **30**(4): p. 669-682.
24. Nakamura, K., M. Matsumoto, and O. Hikosaka, *Reward-Dependent Modulation of Neuronal Activity in the Primate Dorsal Raphe Nucleus.* The Journal of Neuroscience, 2008. **28**(20): p. 5331-5343.
25. Di Matteo, V., et al., *Serotonin control of central dopaminergic function: focus on in vivo microdialysis studies*, in *Progress in Brain Research*, G. Di Giovann, V. Di Matteo, and E. Esposito, Editors. 2008, Elsevier. p. 7-44.
26. Guiard, B.P., et al., *Functional interactions between dopamine, serotonin and norepinephrine neurons: an in-vivo electrophysiological study in rats with monoaminergic lesions*. International Journal of Neuropsychopharmacology, 2008. **11**(5): p. 625-639.
27. Cools, R., K. Nakamura, and N.D. Daw, *Serotonin and Dopamine: Unifying Affective, Activational, and Decision Functions.* Neuropsychopharmacology, 2011. **36**(1): p. 98-113.
28. Li, Y., et al., *Synaptic mechanism underlying serotonin modulation of transition to cocaine addiction.* Science, 2021. **373**(6560): p. 1252-1256.
29. Pelloux, Y., et al., *Reduced forebrain serotonin transmission is causally involved in the development of compulsive cocaine seeking in rats.* Neuropsychopharmacology, 2012. **37**(11): p. 2505-14.
30. Koob, G.F., *Drugs of abuse: anatomy, pharmacology and function of reward pathways.* Trends Pharmacol Sci, 1992. **13**(5): p. 177-84.
31. Dagher, M., et al., *Optogenetic Stimulation of Midbrain Dopamine Neurons Produces Striatal Serotonin Release.* ACS Chem Neurosci, 2022. **13**(7): p. 946-958.
32. Dray, A., et al., *Evidence for the existence of a raphe projection to the substantia nigra in rat.* Brain Research, 1976. **113**(1): p. 45-57.
33. Chang-Tien, T., *Involvement of serotonin in mediation of inhibition of substantia nigra neurons by noxious stimuli.* Brain Research Bulletin, 1989. **23**(1): p. 121-127.
34. Trent, F. and J.M. Tepper, *Dorsal raphé stimulation modifies striatal-evoked antidromic invasion of nigral dopaminergic neurons in vivo.* Exp Brain Res, 1991. **84**(3): p. 620-30.
35. Wang, H.L., et al., *Dorsal Raphe Dual Serotonin-Glutamate Neurons Drive Reward by Establishing Excitatory Synapses on VTA Mesoaccumbens Dopamine Neurons.* Cell Rep, 2019. **26**(5): p. 1128-1142.e7.
36. Ferry, B., et al., *Analysis of microdialysate monoamines, including noradrenaline, dopamine and serotonin, using capillary ultra-high performance liquid chromatography and electrochemical detection.* Journal of Chromatography B, 2014. **951-952**: p. 52-57.
37. Labouesse, M.A., R.B. Cola, and T. Patriarchi, *GPCR-Based Dopamine Sensors-A Detailed Guide to Inform Sensor Choice for In vivo Imaging.* Int J Mol Sci, 2020. **21**(21).
38. Patriarchi, T., et al., *Ultrafast neuronal imaging of dopamine dynamics with designed genetically encoded sensors.* Science, 2018. **360**(6396).

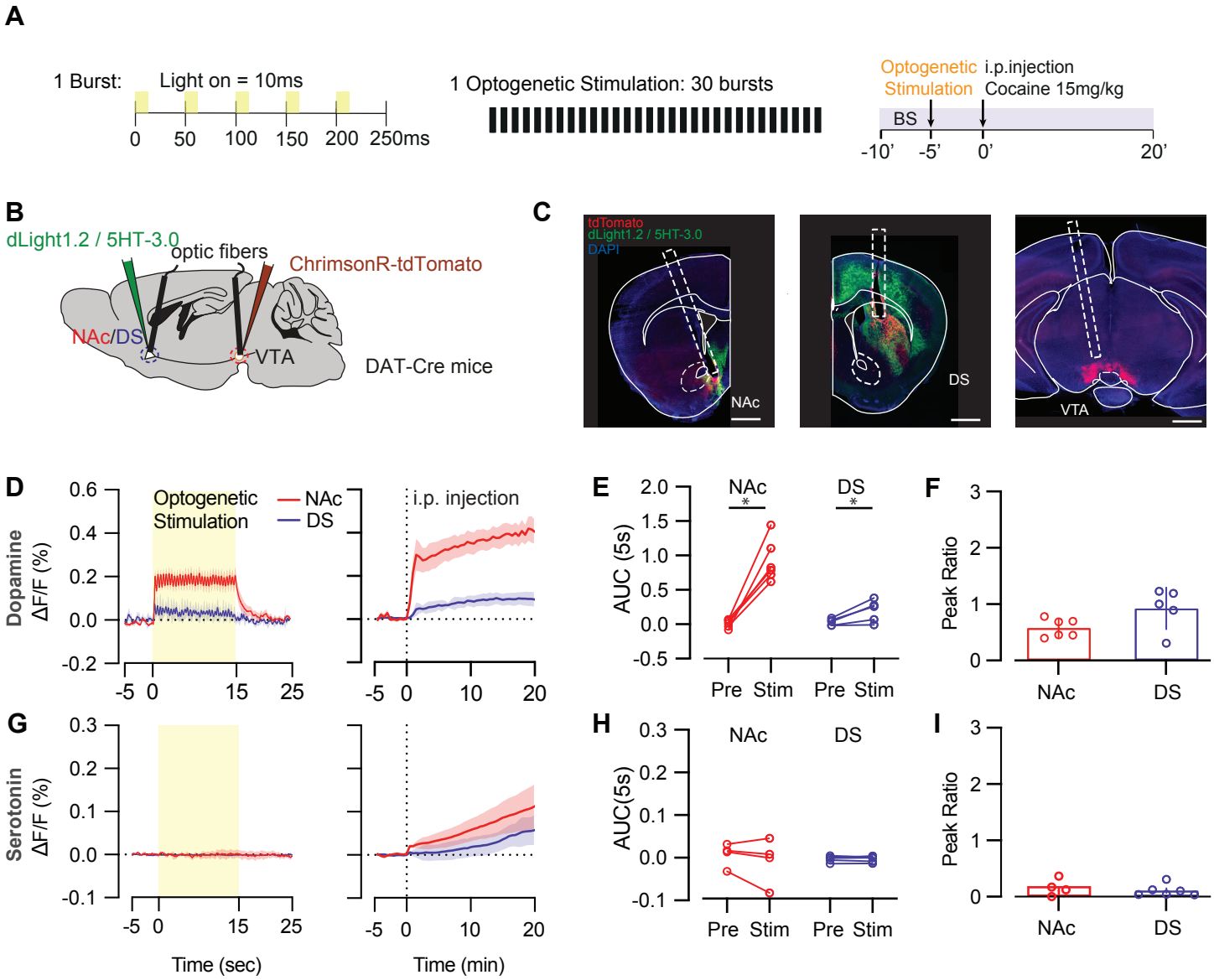
A
1 Burst:
Light on = 10ms
0
50
100
150
200
250ms
1 Optogenetic Stimulation: 30 bursts
Optogenetic Stimulation
i.p.injection Cocaine 15mg/kg
BS
-10'
-5'
0'
20'
B
dLight1.2 / 5HT-3.0
optic fibers
ChrimsonR-tdTomato
NAc/DS
VTA
DAT-Cre mice
C
tdTomato
dLight1.2 / 5HT-3.0
DAPI
NAc
DS
VTA
D
Dopamine
ΔF/F (%)
Optogenetic Stimulation
NAc
DS
i.p. injection
E
AUC (5s)
NAc
DS
Pre
Stim
F
Peak Ratio
NAc
DS
G
Serotonin
ΔF/F (%)
Time (sec)
Time (min)
H
AUC(5s)
NAc
DS
Pre
Stim
I
Peak Ratio
NAc
DS

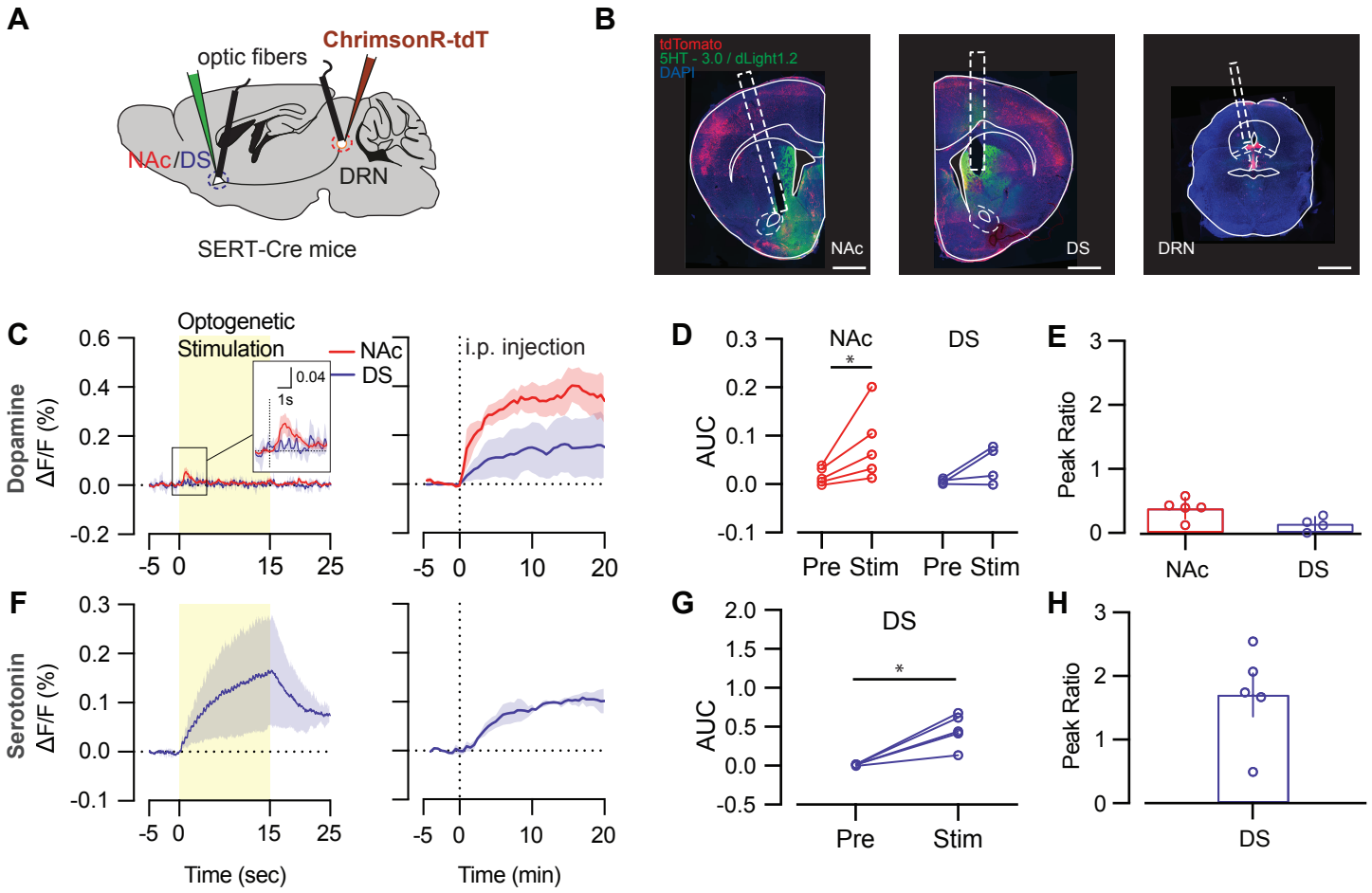
A
optic fibers
ChrimsonR-tdT
NAc/DS
DRN
SERT-Cre mice
B
tdTomato
5HT - 3.0 / dLight1.2
DAPI
NAc
DS
DRN
C
Optogenetic Stimulation
NAc
DS
0.04
1s
i.p. injection
Dopamine ΔF/F (%)
D
NAc
DS
AUC
Pre Stim
Pre Stim
E
Peak Ratio
NAc
DS
F
Serotonin ΔF/F (%)
Time (sec)
Time (min)
G
DS
AUC
Pre
Stim
H
Peak Ratio
DS

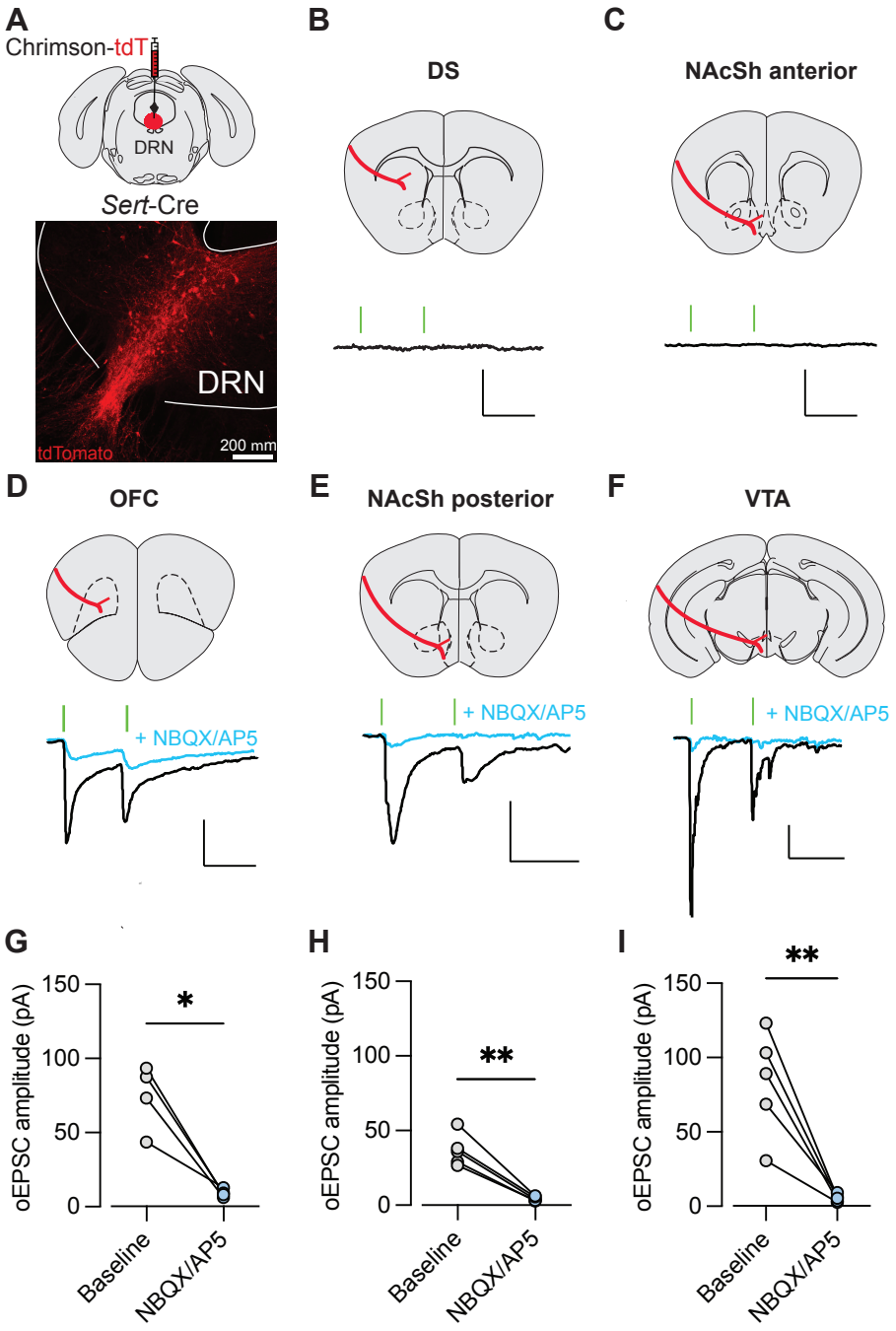
A
Chrimson-tdT
DRN
Sert-Cre
DRN
tdTomato
200 mm
B
DS
C
NAcSh anterior
D
OFC
+ NBQX/AP5
E
NAcSh posterior
+ NBQX/AP5
F
VTA
+ NBQX/AP5
G
oEPSC amplitude (pA)
150
100
50
0
*
Baseline
NBQX/AP5
H
oEPSC amplitude (pA)
150
100
50
0
**
Baseline
NBQX/AP5
I
oEPSC amplitude (pA)
150
100
50
0
**
Baseline
NBQX/AP5